

# A Statistical Modeling Approach to Catalyst Generality Assessment in Enantioselective Synthesis

Junshan Lai, Jiajing Li, Isaiah O. Betinol, Yutao Kuang and Jolene P. Reid\*

Department of Chemistry, University of British Columbia, 2036 Main Mall, Vancouver, British Columbia, V6T 1Z1, Canada

**ABSTRACT:** Selecting the optimal catalyst to impart high levels of enantioselectivity in a new transformation is challenging because the ideal molecular requirements of the catalyst for one reaction do not always simply translate to another. In these reaction scenarios practitioners typically use the most general catalyst structure as a starting point for optimization. However, for many reaction systems and catalyst chemotypes the most general catalyst structure may be largely unknown presenting a significant limitation in catalyst application to new reaction space. Herein, we demonstrate that comprehensive statistical models can be applied to identify the most general catalyst for many chemical systems. These inclusive statistical models that encompass many reaction types can provide information about the relevant structural requirements necessary for high enantioselectivity across a broad reaction range. By validating this approach on diverse regions of organocatalyzed reaction space we discovered structurally distinct catalysts can in some cases provide similar levels of enantioselectivity. The second curious finding determined that the best and most popular catalyst systems may not be equivalent. Validation of this approach on a multi-catalytic dearomatization reaction resulted in the discovery that our general catalyst findings allowed for streamlined reaction development for highly complex transformations.

Synthetic strategies that can be applied to assemble an assortment of chiral molecules without unexpected changes to the experimental outcome are most frequently employed in enantioselective synthesis.<sup>1</sup> The simplicity of the reaction components involved in substrate and reagent control have rendered such protocols to be impressively robust. Accordingly, these methods can be applied to include new and complex substrates with confidence. However, in these mechanistic scenarios one chiral molecule of starting material is consumed to produce a single molecule of product. In contrast, catalytic strategies can be applied more efficiently but often with a lower degree of generality.<sup>2</sup> Hence, the ability to identify general enantioselective catalysts is both necessary and difficult.<sup>3,4</sup>

Forecasting the suitability of an asymmetric catalyst for a particular reaction system is challenging as the optimal molecular features for one transformation do not always translate to another.<sup>5</sup> Furthermore, catalysts that are currently considered as the most “general” may be biased by the existing literature.<sup>6</sup> In other words, catalysts that have provided adequate levels of enantioselectivity in similar reaction systems are likely to be the first used in new reaction spaces.<sup>7</sup> Consequently, the best and most popular catalyst systems may not be equivalent. This issue is further exasperated by the lack of comparative data meaning inferences must be drawn from incomplete data sets generated under non-uniform conditions. Considering these challenges, we hypothesized that a method for predicting the impact of the catalyst structure on the enantioselectivity outcome for a diverse set of transformations could help identify general systems.<sup>8-14</sup> In this context, our group has been focused on developing comprehensive statistical models that connect reaction types by relating the molecular features of all of the reaction components to the experimentally obtained enantioselectivity,  $\Delta\Delta G^\ddagger$  (Figure 1).<sup>15-17</sup>

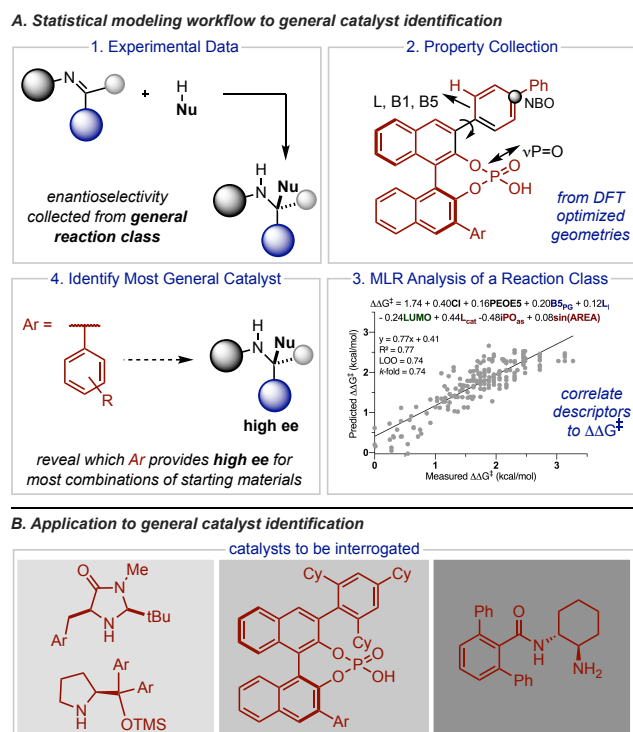


**Figure 1.** (A) Statistical modeling workflow that describe entire reaction classes for the identification of general catalysts. The nucleophilic addition to imines catalyzed by chiral phosphoric acids is shown as an example. (B) Focus of this work is to vet the approach on diverse areas of organocatalysis.

The resulting general relationship determines the structural features necessary for high enantioselectivity while simultane-

ously providing a platform for predicting the impact of reaction components not included in the initial training correlation. These tools have been used for several prediction tasks such as target molecule synthesis<sup>7</sup> and reaction development<sup>18</sup> but have yet to be explored for the identification of general catalysts (Figure 1). As a significant step forward, we evaluated this data-driven workflow as a platform for generality assessment. In contemplating this type of optimization problem, several questions were apparent: (1) considering the diverse catalyst structures employed for organocatalysis, can structurally unique catalysts provide similar levels of generality? (2) Do the most general catalysts translate to the most popular catalyst structures? (3) And lastly, can statistical models identify general catalysts even when different catalyst chemotypes are being interrogated? Herein, we begin to probe these questions by challenging three different statistical models incorporating various catalyst classes with a range of reactants to reveal unexpected generalities in catalyst performance.

**Inverse catalyst design.** To initiate the first part of our study, we selected secondary amines as the platform to assess catalyst performance in diverse reaction space. More specifically, several simple amine structures can catalyze a wide array of bond constructions in high enantioselectivity and many of these reactions have been connected through our groups previous statistical modeling efforts.<sup>19</sup> This published model describes the reaction between aldehydes and a broad range of reactants that proceed *via* chiral iminium/enamine intermediates (Figure 2). With this data set, we set out to uncover whether two structurally unique subclasses of catalysts, imidazolinone and diarylprolinol silyl ethers provide equivalent levels of enantioinduction across a broad reaction range. Although the reasons of stereoinduction are thought to be similar, these catalysts are quite disparate, and a practicing organic

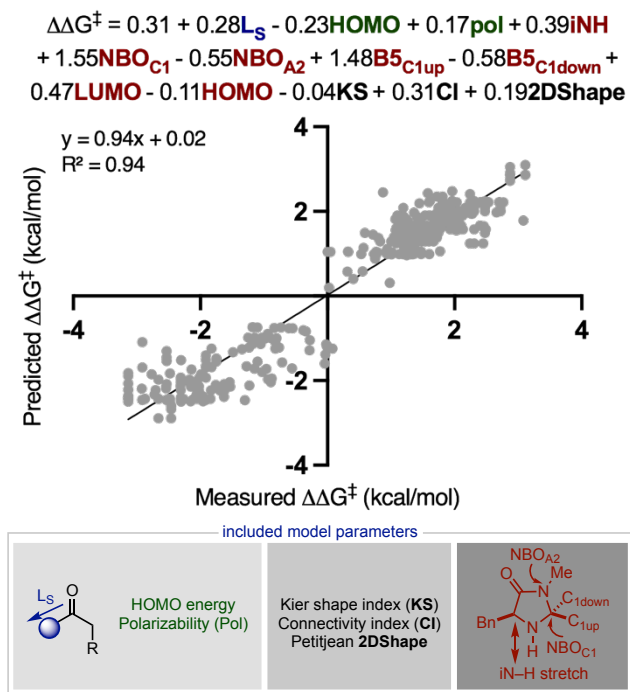
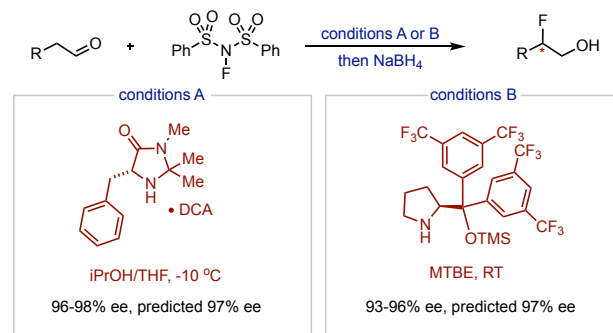


**Figure 2.** Published statistical model for predicting secondary amine catalyzed reactions.<sup>19</sup>

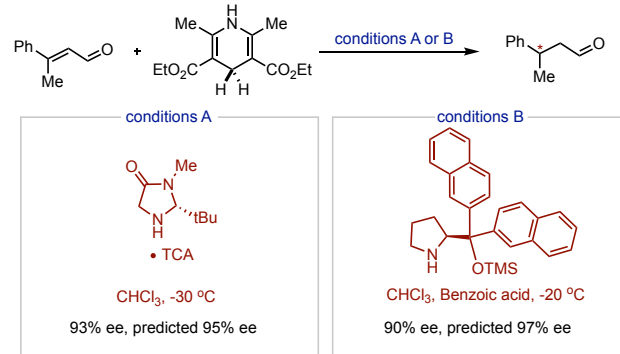
chemist would not necessarily think to substitute one with the other. Consequently, we explored the model's ability to predict a set of aldehyde/reagent combinations that were catalyzed by both amine types and were not included in model. If

effective out-of-sample prediction were possible, the model could provide the necessary data for generality assessment. Because the comparison data is gathered from individual publications the reaction conditions are occasionally different. In many cases, the reaction condition changes are subtle (i.e. one polar solvent for another) so they are similar enough to expect comparable selectivity of the catalysts under each condition. Intriguingly, while both catalysts have been employed to facilitate similar reactions and are commercially available, they are rarely included in the same catalyst screen. This makes it difficult to build powerful mechanistic connections between the two catalyst subclasses. As a first evaluation, the fluorination of aldehydes using NFSI was predicted with the optimal conditions found for each subclass of amine (Figure 3A).<sup>20,21</sup>

**A. Assessing different amine subclasses for fluorination of aldehydes**



**B. Predicting transfer hydrogenation reactions common to both amines**



**C. Exploring amination reactions not included in the training data**

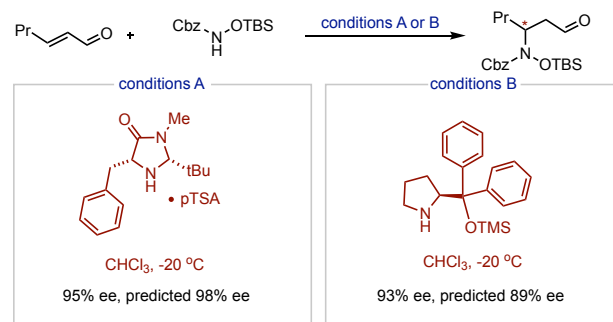


**Figure 3A-C.** Diverse secondary amines provide comparable levels of enantioselectivity. Because different absolute product stereochemistry is reported in some examples, we have not included this information.

This test set included three substrates common to both catalysts. Prior to submitting the relevant model descriptors collected from each reaction component, these specific combinations of aldehyde and NFSI were removed from the training set. The model was then updated and deployed to predict the reaction outcomes (see SI for more information). Because this

aldehyde substrate was highly represented in the training set the model accurately predicts the results. Through further assessment we found that the model can also accurately predict the outcome of Hantzsch ester hydrogenations common to both amines (Figure 3B).<sup>22,23</sup> In the next set of evaluations, we determined the model's ability to predict amination reactions.<sup>24,25</sup> These test cases include new reactants and consequently, are predicted using the full training set shown in Figure 2. As with the other cases, only a small set of overlapping reactions were available for testing but were accurately predicted by the model (Figure 3C).

In each of the examples, the model correctly anticipates that both catalysts generate products with similarly high levels of enantioselectivity. This factor combined with the model accuracy suggests that the statistical model can be used to probe the impact of the two amines more comprehensively. However, since the model lacks substrate-catalyst interaction terms the model will constantly predict similar enantioselectivities for both catalyst systems. This is intriguing given that diarylprolinol silyl ethers compared to imidazolininones, have much larger steric bulk next to site of condensation, a structural feature important for high enantioselectivity. On this basis, it is superficially surprising that imidazolininones should perform so well, the model reveals through examination of the parameters that the more positive  $NBO_{Cl}$  largely compensate for the smaller  $B5_{Cl_{up}}$ . By further analyzing the terms included in the statistical model, the performance of diarylprolinol silyl ethers can be attributed to the more negative  $NBO_{Cl}$  which overrides any beneficial impact garnered from the large  $B5_{Cl_{up}}$ . These features have the net result that two structurally diverse catalysts perform comparably across a wide range of enantioselective bond constructions.<sup>26</sup> Such mechanistic insight is unique to comprehensive statistical models which reveal the important molecular features for catalyst performance across a reaction range. Nonlinear dimensionality reduction techniques like PCA can be employed to cluster compounds with similar properties but because these do not take account the relative parameter importance these fail in this case to identify the interconnectivity between the amine subclasses (see SI).<sup>27,28</sup>

**Literature popular catalysts.** To further establish the workflow for generality assessment, we explored the possibility of the model to identify catalysts that lead to a better performance than those considered most popular. Accordingly, we sought to vet the workflow against known catalyst systems that have been broadly applied. Given the recorded frequency of chiral phosphoric acids employed in the asymmetric synthesis of various organic compounds, this catalyst class served as a prime example.<sup>29</sup> As proof of concept, we have re-examined the nucleophilic additions to *E*-imines catalyzed by chiral phosphoric acids, which was utilized during the course of one of the authors efforts to correlate entire reaction classes.<sup>5</sup> In these examples, TRIP, which has large isopropyl groups at the 2,4,6 positions of the aromatic ring, has been commonly found to be the optimal catalyst. However, we questioned if TCYP, a more recently discovered but structurally similar catalyst might provide higher enantioselectivities across a broader set of reactions. Because TCYP has not been used in the development of these reactions, implicit chemical data on applying this catalyst is sparse. By leveraging the previously built statistical model we can anticipate how TCYP would perform in various nucleophilic additions to *E*-imines.

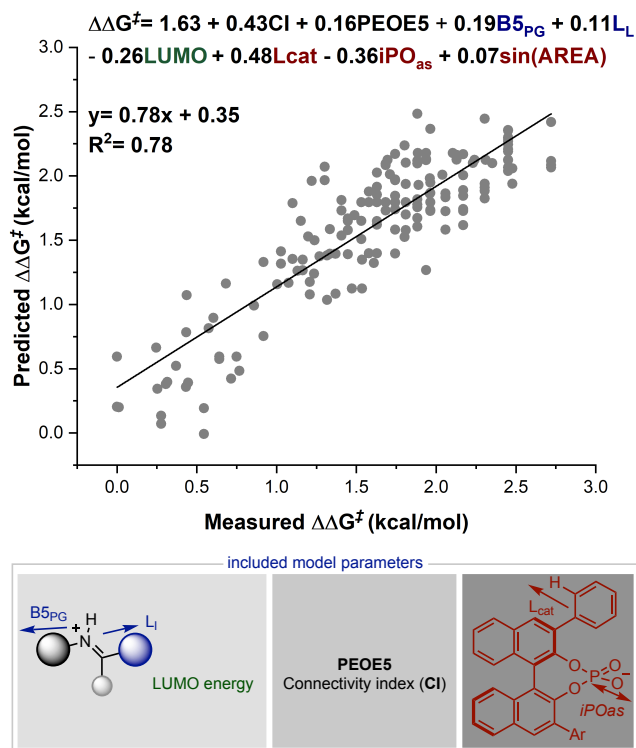


**Figure 4.** Published statistical model for predicting chiral phosphoric acid catalyzed reactions involving *E*-imines and protic nucleophiles.

The results from these predictions would in turn provide the comparison data necessary for this analysis. Therefore, the goal of the prediction analysis is to identify general catalyst trends across reactions rather than distinguish between subtleties of substrate-dependent enantioselectivity. When the enantioselectivity is high, as is typically the case for TRIP and TCYP, evaluation metrics like average prediction error are less important than the number of higher selectivity reactions a catalyst provides over another.

As the initial test study we utilized the addition of thiols to benzoyl imines reported by Antilla.<sup>30</sup> To test our hypothesis that TCYP is a more general catalyst, all experimental results of this reaction catalyzed by TRIP were removed from the original training set. The model was retrained, and deployed to predict 25 reaction outcomes with TRIP and TCYP. A summary of the predictions obtained from the model are shown in Figure 4 alongside the experimental results that were reported separately by Denmark.<sup>31</sup> For each reaction example the model predicts TCYP will provide higher enantioselectivities than TRIP. Crucially, this predicted trend closely resembles the experimental results with only 5 out of the 25 recorded examples show TRIP to be more selective. Considering the logarithmic function of  $\Delta\Delta G^\ddagger$ , the differences between catalyst performance can appear small. In one example, the experimental change is only 10% ee (predicted 4% ee) which corresponded to a free energy difference of 0.77 kcal/mol (predicted 0.80 kcal/mol). To put this metric into perspective, adjusting the catalyst from TRIP to TCYP could have a dramatic and positive impact on less selective reactions. Combining these successful results with an analysis of the included parameters (i.e. no catalyst-substrate interaction terms present)

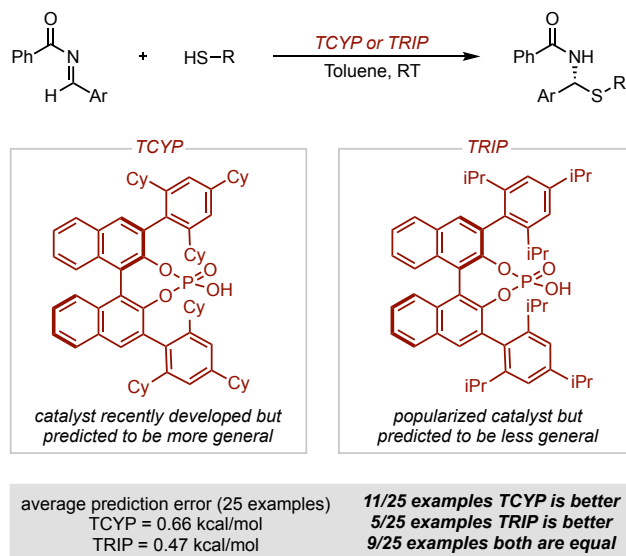


**Figure 4.** Predicting the performance of TCYP and TRIP in an acid catalyzed thiol addition to imines.

implies that this model will always predict TCYP to outperform TRIP. Where additional comparison data is available, several other studies involving imine-type electrophiles (C=N-R) have shown the importance of including TCYP in a catalyst evaluation despite the structural similarities with TRIP.<sup>32-41</sup> By performing this type of analysis with similarly related electrophiles, azo compounds,<sup>42-46</sup> precedent shows TCYP to be a top performer. Continued expansion of this comparative analysis demonstrates TCYP to be effective in condensation,<sup>47,48</sup> halogenation<sup>49-52</sup> and organometallic reactions.<sup>53-57</sup> This list can be even further extended to include more mechanistically disparate reactions.<sup>58-65</sup> However, like the thiol addition reaction described in Figure 4 in some cases TRIP provides better<sup>66-73</sup> or the same levels of enantioselectivity.<sup>74,75</sup> The translation of this trend beyond reactions involving imines strongly implies that including TCYP in the first round of catalyst screening for any given system would increase the probability of achieving a successful result. To further explore this idea in new reaction space we decided to compare the performance of TCYP and TRIP in a gold-catalyzed dearomatization reaction involving indole as the nucleophile (Table 1). This protocol has been reported to work well with 2-naphthols and 9-anthryl derived chiral phosphoric acid catalysts but there is little information on how other catalysts and nucleophiles would react.<sup>76</sup> Therefore, this platform provides the ideal opportunity to test our hypothesis beyond what is included in the model while allowing the reaction scope to be meaningfully extended in the process. It should be noted that this reaction can be performed solely with a Brønsted acid but the reaction requires very high molecular weight catalysts to achieve excellent levels of enantioselectivity and some substrates perform less well.<sup>77</sup> Beyond the noted limitations in the reported methodology part of our motivation to focus on complex multi-catalysis protocols is embedded in the difficulty in applying these reaction types to enantioselective synthesis. Because these systems require the optimization of two catalyst structures (as well as other parameters) we postulated that knowing the most general catalyst of the chiral component to be applied would significantly reduce the barrier to reaction optimization.

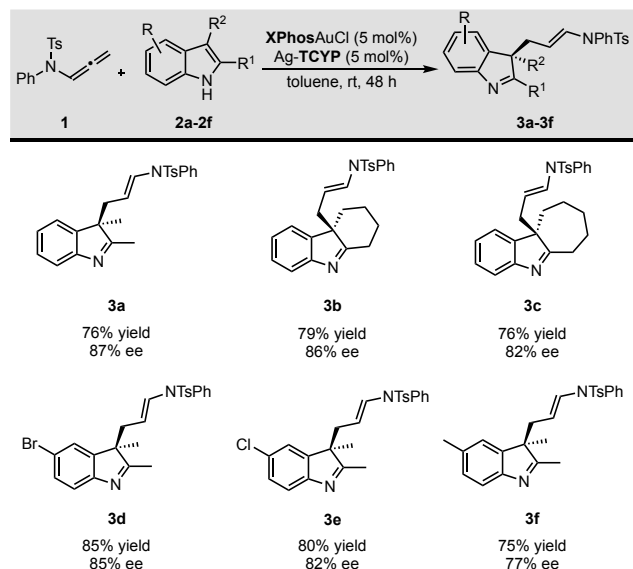
**Table 1.** Testing the effect of chiral phosphoric acid and gold phosphine catalysts<sup>a</sup>

entry	CPA	L	Yield <sup>b</sup> (%)	ee <sup>c</sup> (%)
1	TRIP	PPh <sub>3</sub>	67	57
2	TCYP	PPh <sub>3</sub>	70	60
3	TCYP	JohnPhos	75	81
4	TCYP	XPhos	76	87
5	TCYP	<sup>t</sup> BuXPhos	70	85
6	TCYP	–	70	72

<sup>a</sup>Unless otherwise noted, reactions were run with the following conditions: Allene substrate (0.1 mmol), indole (0.2 mmol), gold phosphine (5 mol%), chiral silver phosphate (5 mol%), toluene (1 mL), rt, 48 h. <sup>b</sup>Isolated yields given. <sup>c</sup>Enantioselectivities (ee) were measured by SFC. Absolute configurations assigned based on comparison of optical rotations to published data. See the Supporting Information for further details.

As the first step in testing our ideas, we explored how TRIP and TCYP would perform in the reaction between 2,3-dimethylindole and *N*-phenyl-*N*-sulfonylallenamide. Intriguingly, the catalyst trends translated to this complex multi-catalyst protocol with TRIP proceeding in 57% ee and TCYP 60% ee (Table 1 entries 1 and 2). Based on our analysis, TCYP was likely to be the best chiral phosphoric acid performer; thus, to increase the enantioselectivity of the reaction we focused on modifying the phosphine ligand. Johnphos was identified as the optimal ligand in the reaction involving 2-naphthol derivatives and in our system, this also performed well providing the product in 81% ee (Table 1 entry 3). Increasing the steric profile of the ligand increased the enantioselectivity even further with XPhos providing the product in 87% ee (Table 1 entry 4). This is slightly more selective than the single catalyst system employing TCYP only (84% ee), although this previously reported result was performed in slightly different conditions (benzene as the solvent).<sup>77</sup> To accurately gauge the effectiveness of this multi-catalysis protocol we performed the reaction involving TCYP as the sole catalyst and used toluene as the solvent. Intriguingly the product was obtained in only 72% ee (Table 1 entry 6), meaning that under otherwise identical conditions, adding a gold phosphine boosts the ee by 15%. The scope of the reaction was tested to include a set of six diverse indoles (Scheme 2). These performed with similar levels of enantioselectivity and reactivity. Importantly, we were able to increase the enantioselectivity of a substrate that previously performed poorly under the acid only conditions to 77% ee as compared to the formerly reported value of 72% ee.<sup>77</sup> Ultimately, this example showcases that having knowledge about the most general catalysts can streamline reaction development even in complex multi-catalysis protocols. Further, based on these results it is our recommendation that TRIP cannot act as a replacement for TCYP and that both catalysts should be included in reaction optimizations.

**Table 2.** Various indoles tested with the optimized multicatalytic protocol.<sup>a</sup>



<sup>a</sup>Reaction conditions: Allene substrate (0.1 mmol), indole (0.2 mmol), XPhosAuCl (5 mol%), Ag-TCYP (5 mol%), toluene (1 mL), rt, 48 h. Isolated yields given. Enantioselectivities (ee) were measured by HPLC or SFC. Absolute configurations assigned based on comparison of optical rotations to published data. See the Supporting Information for further details.

**Multiple catalyst chemotypes.** Finally, we aimed to demonstrate that our statistical workflow can identify general catalysts from a diverse pool of potential structures. To accomplish this, we inverted the subject of the analysis to multiple catalyst chemotypes incorporating different elements of molecular recognition. Considering the model was to be developed to encompass many catalyst types, we determined the fluorination of branched aldehydes provided the requisite structural diversity and data spread required for statistical analysis. Specifically, primary and secondary amines can facilitate this reaction with varying levels of enantioselectivity spanning a selectivity window of 99% ee. A total of 68 reactions from four publications were curated for statistical modeling which included eight catalyst types ranging from simple chiral amines with single stereocenters to more complex systems that can enable a diverse set of substrate-catalyst contacts.<sup>78-81</sup> The complexity of the catalyst structures limited our ability to encode product configurations, meaning absolute enantioselectivities were employed as the experimental output. This requirement was necessary for eliminating bias and useful for producing a well-distributed data set. Following data gathering, a diverse array of molecular descriptor values was collected from DFT optimized geometries to describe the structural features of each aldehyde, fluorinating reagent, catalyst and solvent.<sup>82</sup> This parameter set consisting of Sterimol size descriptors, NBO charges, IR vibrations, polarizability, HOMO and LUMO energies was assimilated from the ground state conformation of each calculated reaction component. Solvent effects were described by topological, two-dimensional descriptors typically employed for QSAR modeling of structurally disparate molecules (e.g., molecular shape, size and the number of heteroatoms). Other reaction variables like concentration of reagents/catalyst were included as numerical parameters. Because the goal is to imitate the workflow traditionally employed in catalyst generality assessment,

a set of overlapping aldehyde/reagent combinations between the publications were removed prior to correlating building.<sup>78,81</sup> Using forward stepwise linear regression in MATLAB, a pool of prospective models were generated. Since the model was to be applied to predict the impact of diverse catalyst structures only models containing catalyst terms were selected for evaluation. Using this as the basis for model selection, the pool was further refined by R<sup>2</sup> and parameter number. By considering these criteria, we determined a seven-parameter model exhibiting a high R<sup>2</sup> value and validation scores to be ideal for our predictive purposes (see SI for further details). The general relationship included four aldehyde, one reagent, catalyst and solvent parameters. Specifically, large aldehyde substituents were typically important for high enantioselectivities. This is congruent with the hypothesis that energetically repulsive steric interactions likely between catalyst and substrate has the result of disfavoring the transition state leading to the minor enantiomer. The inclusion of reagent concentration with a negative coefficient implies that excess reagent may facilitate erosion of enantioselectivity (Figure 5).

The next step in assessing our model was to test the ability of extrapolating to aldehyde/fluorination combinations not included in the model development process. This was accomplished by predicting the enantioselectivity of 10 unique pairings catalyzed by two different primary amines.<sup>78,81</sup> Each result was predicted using the model, with an average

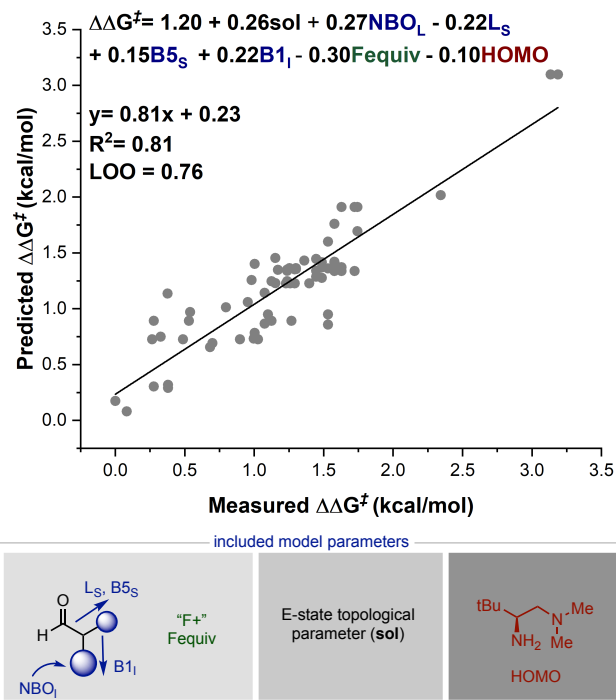


**Figure 5.** Statistical model correlating the enantioselectivity of amine catalyzed fluorination of branched aldehydes.

absolute  $\Delta\Delta G^\ddagger$  error of 0.14 and 0.25 kcal/mol for the two catalyst subclasses, demonstrating the ability of the model to extrapolate effectively to new substrates. The low prediction error obtained for both systems translated to the correct identification of both catalysts **4** and **5** to be equivalently selective across a broad range of substrates (see Figure 6 for examples). Of particular note was the model's ability to predict the best (86% ee) and poorest (48% ee) result with catalyst **5** to within

3% ee. This successful result prompted us to continue to challenge the models predictive capabilities to include more complex catalyst types which may exhibit greater substrate generalities than those included in the training set. Accordingly, the next prediction platform featured a new catalyst type with molecular properties that were quite dissimilar to the training set. This final test study assessed a BINOL-derived primary amine as the catalyst with large aromatic groups at the 3,3' positions of the binaphthyl backbone.<sup>83</sup> In contrast to the previous catalysts discussed, this system is C<sub>2</sub> symmetric and displays axial chirality. Considering the general catalyst features required for high enantioselectivity were conserved (negative HOMO), we reasoned that extrapolation to new chiral scaffolds should not lead to large errors in predicting ee. Indeed, accurate predictions were construed with the statistical model with an average absolute  $\Delta\Delta G^\ddagger$  error of 0.25 kcal/mol across 5 substrates that were not included in the training set and overlapped with both catalyst 4 and 5. This example serves to highlight that the model can extrapolate to catalysts encompassing different chiral elements. When assessing this system the model predicted some of the highest enantioselectivities reported, a result of decreasing the catalyst HOMO energy. For the substrates shown in Figure 6, the model predicts the catalyst to increase in selectivity by about 0.20 kcal/mol (around 8% ee) as compared to the other two primary amines.

Therefore, with no experimental data on this catalyst, the model accurately captured this primary amine, catalyst 6, as the most selective across the overlapping reactant space.

## CONCLUSION

General or “privileged catalysts” are immensely valuable for both enantioselective method development and application to complex, chiral molecule synthesis. Yet, predicting how general an asymmetric catalyst could be is still an extremely difficult task. Here, we show that comprehensive statistical models that encompass many different reaction types can be successfully applied to predict catalysts that work well across diverse reaction space. Specifically, we demonstrated that these statistical modeling tools were able to identify general chiral phosphoric acid, primary and secondary amine organocatalysts. Further, we reveal how our findings can inform catalyst selection and facilitate the optimization of a complex multicatalytic reaction to obtain chiral indolines. Overall, we believe that our approach should be relevant and valuable for the prediction and identification of other general catalytic systems.

## Supporting Information

The Supporting Information is available free of charge. Experimental procedures, characterization data, computational and statistical modeling details (PDF)

## AUTHOR INFORMATION

### Corresponding Author

\*jreid@chem.ubc.ca

## ACKNOWLEDGMENT

Financial support to J.P.R is provided by the University of British Columbia and the Natural Sciences and Engineering Research Council of Canada (NSERC). J.L thanks the University of British Columbia for a 4Y scholarship. I.O.B acknowledges NSERC for a CGSM research fellowship. Y.K. thanks the Chinese Scholarship Council (CSC) for a graduate research fellowship. Computational resources were provided from Compute Canada and the Advanced Research Computing (ARC) center at the University of British Columbia.

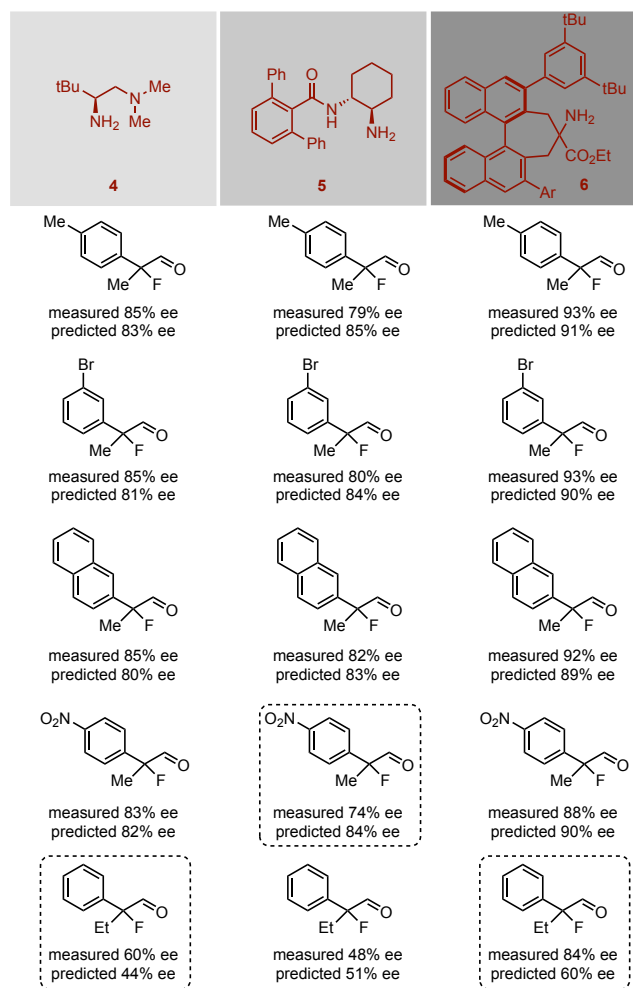


**Figure 6.** The model correctly identifies catalyst 6 to be most selective across the overlapping substrate range. Examples that had errors larger than 6% ee are highlighted by a dashed box.

## REFERENCES

- (1) Reid, J. P. Open questions on the transfer of chirality. *Commun Chem* **2021**, *4*, 171.
- (2) Strassfeld, D. A.; Algera, R. F.; Wickens, Z. K.; Jacobsen, E. N. A case study in catalyst generality: simultaneous, highly-enantioselective Brønsted- and Lewis-acid mechanisms in hydrogen-bond-donor catalyzed oxetane openings. *J. Am. Chem. Soc.* **2021**, *143*, 9585–9594.
- (3) Prieto Kullmer, C. N.; Kautzky, J. A.; Krska, S.W.; Nowak, T.; Dreher, S. D.; MacMillan, D.W.C. Accelerating reaction generality and mechanistic insight through additive mapping. *Science*. **2022** *376*, 532–539.
- (4) Wagen, C. C.; McMinn, S. E.; Kwan, E. E.; Jacobsen, E. N. Screening for Generality in Asymmetric Catalysis; *ChemRxiv*, **2022**.
- (5) Reid, J. P.; Sigman, M. S. Holistic prediction of enantioselectivity in asymmetric catalysis. *Nature* **2019**, *571*, 343–348.
- (6) Beker, W.; Roszak, R.; Wołos, A.; Angello, N. H.; Rathore, V.; Burke, M. D.; Grzybowski, B. A. Machine Learning May Sometimes Simply Capture Literature Popularity Trends: A Case Study of Heterocyclic Suzuki-Miyaura Coupling. *J. Am. Chem. Soc.* **2022**, *144*, 4819–4827
- (7) Betinol, I. O.; Kuang, Y.; Reid, J. P. Guiding Target Synthesis with Statistical Modeling Tools: A Case Study in Organocatalysis. *Org. Lett.* **2022**, *24*, 1429–1433.
- (8) Rinehart, N. I.; Zahrt, A. F.; Henle, J. J.; Denmark, S. E. Dreams, False Starts, Dead Ends, and Redemption: A Chronicle of the Evolution of a Chemoinformatic Workflow for the Optimization of Enantioselective Catalysts. *Acc. Chem. Res.* **2021**, *54*, 2041–2054.
- (9) Żurański, A. M.; Martínez Alvarado, J. I.; Shields, B. J.; Doyle, A. G. Predicting Reaction Yields via Supervised Learning. *Acc. Chem. Res.* **2021**, *54*, 1856–1865.
- (10) Crawford, J. M.; Kingston, C.; Toste, F. D.; Sigman, M. S. Data Science Meets Physical Organic Chemistry. *Acc. Chem. Res.* **2021**, *54*, 3136–3148.
- (11) Laplaza, R.; Gallarati, S.; Corminboeuf, C. Genetic Optimization of Homogeneous Catalysts. *Chem.–Methods*, **2022**, *2*, e20210010.
- (12) Jorner, K.; Tomberg, A.; Bauer, C.; Sköld, C.; Norrby, P.-O. Organic Reactivity from Mechanism to Machine Learning. *Nat. Rev. Chem.* **2021**, *5*, 240–255
- (13) Keith, J. A.; Vassilev-Galindo, V.; Cheng, B.; Chmiela, S.; Gastegger, M.; Müller, K.-R.; Tkatchenko, A. Combining Machine Learning and Computational Chemistry for Predictive Insights Into Chemical Systems. *Chem. Rev.* **2021**, *121*, 9816–9872
- (14) Lustosa, D. M.; Milo, A. Mechanistic Inference from Statistical Models at Different Data-Size Regimes. *ACS Catal.* **2022**, *12*, 7886–7906.
- (15) Shoja, A.; Reid, J. P. Computational Insights into Privileged Stereocontrolling Interactions Involving Chiral Phosphates and Iminium Intermediates. *J. Am. Chem. Soc.* **2021**, *143*, 7209–7215.
- (16) Shoja, A.; Zhai, J.; Reid, J. P. Comprehensive Stereochemical Models for Selectivity Prediction in Diverse Chiral Phosphate-Catalyzed Reaction Space. *ACS Catal.* **2021**, *11*, 11897–11905.
- (17) Betinol, I. O.; Reid, J. P. A predictive and mechanistic statistical modelling workflow for improving decision making in organic synthesis and catalysis. *Org. Biomol. Chem.* **2022**, *20*, 6012–6018.
- (18) Reid, J. P.; Proctor, R. S. J.; Sigman, M. S.; Phipps, R. J. Predictive Multivariate Linear Regression Analysis Guides Successful Catalytic Enantioselective Minisci Reactions of Diazines. *J. Am. Chem. Soc.* **2019**, *141*, 19178–19185.
- (19) Kuang, Y.; Reid, J. P. Transferable Selectivity Profiles Enable Prediction in Synergistic Catalyst Space. *ChemRxiv* **2021**, DOI: 10.26434/chemrxiv-2021-q5n18
- (20) Marigo, M.; Fielenbach, D.; Braunton, A.; Kjærsgaard, A.; Jørgensen, K. A. Enantioselective Formation of Stereogenic Carbon Fluorine Centers by a Simple Catalytic Method. *Angew. Chem., Int. Ed.* **2005**, *44*, 3703–3706.
- (21) Beeson, T. D.; MacMillan, D. W. Enantioselective organocatalytic  $\alpha$ -fluorination of aldehydes. *J. Am. Chem. Soc.* **2005**, *127*, 8826–8828.
- (22) Ouellet, S. G.; Tuttle, J. B.; MacMillan, D. W. C. Enantioselective Organocatalytic Hydride Reduction. *J. Am. Chem. Soc.* **2005**, *127*, 32–33.
- (23) Zhao, G.-L.; Córdova, A. Direct organocatalytic asymmetric reductive Mannich-type reactions. *Tetrahedron Lett.* **2006**, *47*, 7417–7421.
- (24) Vesely, J.; Ibrahim, I.; Rios, R.; Zhao, G.-L.; Xu, Y.; Córdova, A. Enantioselective organocatalytic conjugate addition of amines to  $\alpha,\beta$ -unsaturated aldehydes: one-pot asymmetric synthesis of  $\beta$ -amino acids and 1,3-diamines. *Tetrahedron Lett.* **2007**, *48*, 2193–2198.
- (25) Chen, Y. K.; Yoshida, M.; MacMillan, D. W. C. Enantioselective Organocatalytic Amine Conjugate Addition. *J. Am. Chem. Soc.* **2006**, *128*, 9328–9329.
- (26) Kwon, Y.; Li, J.; Reid, J. P.; Crawford, J. M.; Jacob, R.; Sigman, M. S.; Toste, F. D.; Miller, S. J. Disparate Catalytic Scaffolds for Atroposelective Cyclodehydration. *J. Am. Chem. Soc.* **2019**, *141*, 6698–6705.
- (27) Durand, D. J.; Fey, N. Building a Toolbox for the Analysis and Prediction of Ligand and Catalyst Effects in Organometallic Catalysis. *Acc. Chem. Res.* **2021**, *54*, 837–848.
- (28) Gensch, T.; dos Passos Gomes, G.; Friederich, P.; Peters, E.; Gaudin, T.; Pollice, R.; Jorner, K.; Nigam, A.; Lindner-D’Addario, M.; Sigman, M. S.; Aspuru-Guzik, A. A Comprehensive Discovery Platform for Organophosphorus Ligands for Catalysis. *J. Am. Chem. Soc.* **2022**, *144*, 1205–1217.
- (29) Parmar, D.; Sugiono, E.; Raja, S.; Rueping, M. Complete field guide to asymmetric BINOL-phosphate derived Brønsted acid and metal catalysis: history and classification by mode of activation; Brønsted acidity, hydrogen bonding, ion pairing, and metal phosphates. *Chem. Rev.* **2014**, *114*, 9047–9153.
- (30) Ingle, G. K.; Mormino, M. G.; Wojtas, L.; Antilla, J. C. Chiral Phosphoric Acid-Catalyzed Addition of Thiols to N-Acyl Imines: Access to Chiral N, S-Acetals. *Org. Lett.* **2011**, *13*, 4822–4825.
- (31) Zahrt, A. F.; Henle, J. J.; Rose, B. T.; Wang, Y.; Darrow, W. T.; Denmark, S. E. Prediction of Higher-Selectivity Catalysts by Computer-Driven Workflow and Machine Learning. *Science* **2019**, *363*, eaau5631 DOI: 10.1126/science.aau5631
- (32) Tang, M.; Gu, H.; He, S.; Rajkumar, S.; Yang, X. Asymmetric Enamide–Imine Tautomerism in the Kinetic Resolution of Tertiary Alcohols. *Angew. Chem., Int. Ed.* **2021**, *60*, 21334–21339.
- (33) Romano, C.; Jia, M.; Monari, M.; Manoni, E. and Bandini, M. Metal-free enantioselective electrophilic activation of allenamides: stereoselective dearomatization of indoles. *Angew. Chem., Int. Ed.* **2014**, *53*, 13854–13857.
- (34) Sendra, J.; Reyes, E.; Prieto, L.; Fernández, E.; Vicario, J. L. Transannular Enantioselective (3+2) Cycloaddition of Cycloalkenone Hydrazones under Brønsted Acid Catalysis. *Org. Lett.* **2021**, *23*, 8738–8743.
- (35) Zhao, Y.; Cai, L.; Huang, T.; Meng, S.; Chan, A. S.; Zhao, J. Solvent-Mediated C3/C7 Regioselective Switch in Chiral Phosphoric Acid-Catalyzed Enantioselective Friedel-Crafts Alkylation of Indoles with  $\alpha$ -Ketiminooesters. *Adv. Synth. Catal.* **2020**, *362*, 1309–1316.
- (36) Proctor, R. S.; Davis, H. J.; Phipps, R. J. Catalytic enantioselective Minisci-type addition to heteroarenes. *Science* **2018**, *360*, 419–422.
- (37) Wang, Y.; Wang, Q.; Zhu, J. Organocatalytic nucleophilic addition of hydrazones to imines: synthesis of enantioenriched vicinal diamines. *Angew. Chem., Int. Ed.* **2017**, *56*, 5612–5615.
- (38) Cai, Y.; Gu, Q.; You, S. L. Chemoselective N–H functionalization of indole derivatives via the Reissert-type reaction catalyzed by a chiral phosphoric acid. *Org. Biomol. Chem.* **2018**, *16*, 6146–6154.
- (39) Liu, M.; Qian, C.; Li, P. Organocatalytic Regio- and Enantioselective N-Alkylation of Isoxazol-5-ones. *Eur. J. Org. Chem.* **2021**, *2021*, 6777–6780.
- (40) Jin, Y.; Honma, Y.; Morita, H.; Miyagawa, M.; Akiyama, T. Enantioselective Synthesis of 1-Substituted 1, 2, 3, 4-Tetrahydroisoquinolines through 1, 3-Dipolar Cycloaddition by a Chiral Phosphoric Acid. *Synlett* **2019**, *30*, 1541–1545.

- (41) Kim, A.; Kim, A.; Park, S.; Kim, S.; Jo, H.; Ok, K. M.; Lee, S. K.; Song, J.; Kwon, Y. Catalytic and Enantioselective Control of the C–N Stereogenic Axis via the Pictet–Spengler Reaction. *Angew. Chem., Int. Ed.* **2021**, *60*, 12279–12283.
- (42) Guo, Z.; Xie, J.; Hu, T.; Chen, Y.; Tao, H.; Yang, X. Kinetic resolution of N-aryl  $\beta$ -amino alcohols via asymmetric aminations of anilines. *Chem. Commun.* **2021**, *57*, 9394–9397.
- (43) Miles, D. H.; Guasch, J.; Toste, F. D. A nucleophilic strategy for enantioselective intermolecular  $\alpha$ -amination: Access to enantioenriched  $\alpha$ -arylamino ketones. *J. Am. Chem. Soc.* **2015**, *137*, 7632–7635.
- (44) Xie, J.; Guo, Z.; Liu, W.; Zhang, D.; He, Y. P.; Yang, X. Kinetic Resolution of 1, 2-Diamines via Organocatalyzed Asymmetric Electrophilic Aminations of Anilines. *Chin. J. Chem.* **2022**, *40*, 1674–1680.
- (45) Nelson, H. M.; Patel, J. S.; Shunatona, H. P.; Toste, F. D. Enantioselective  $\alpha$ -amination enabled by a BINAM-derived phase-transfer catalyst. *Chem. Sci.* **2015**, *6*, 170–173.
- (46) Qiu, X. Y.; Li, Z. H.; Zhou, J.; Lian, P. F.; Dong, L. K.; Ding, T. M.; Bai, H. Y.; Zhang, S. Y. Chiral Phosphoric Acid-Catalyzed Enantioselective Dearomative Electrophilic Hydrazination: Access to Chiral Aza-Quaternary Carbon Indolenines. *ACS Catal.* **2022**, *12*, 7511–7516.
- (47) Yang, B.; Dai, J.; Luo, Y.; Lau, K. K.; Lan, Y.; Shao, Z.; Zhao, Y. Desymmetrization of 1, 3-diones by catalytic enantioselective condensation with hydrazine. *J. Am. Chem. Soc.* **2021**, *143*, 4179–4186.
- (48) Jiang, Q.; Qin, T.; Yang, X. Asymmetric Synthesis of Hydroquinazolines Bearing C4-Tetrasubstituted Stereocenters via Kinetic Resolution of  $\alpha$ -Tertiary Amines. *Org. Lett.* **2022**, *24*, 625–630.
- (49) Shunatona, H. P.; Früh, N.; Wang, Y. M.; Rauniyar, V.; Toste, F. D. Enantioselective Fluoroamination: 1, 4-Addition to Conjugated Dienes Using Anionic Phase-Transfer Catalysis. *Angew. Chem., Int. Ed.* **2013**, *52*, 7724–7727.
- (50) Phipps, R. J.; Toste, F. D. Chiral anion phase-transfer catalysis applied to the direct enantioselective fluorinative dearomatization of phenols. *J. Am. Chem. Soc.* **2013**, *135*, 1268–1271.
- (51) Xiong, H.; Yoshida, K.; Okada, K.; Ueda, H.; Tokuyama, H. Catalytic Enantioselective 5-endo-Bromocycloetherification of Unactivated Cyclic Alkenes. *Tetrahedron Lett.* **2022**, 153906.
- (52) Rajkumar, S.; He, S. and Yang, X. Kinetic Resolution of Tertiary 2-Alkoxy-carboxamido-Substituted Allylic Alcohols by Chiral Phosphoric Acid Catalyzed Intramolecular Transesterification. *Angew. Chem., Int. Ed.* **2019**, *58*, 10315–10319.
- (53) Zhang, P.; Xing, M.; Guan, Q.; Zhang, J.; Zhao, Q.; Zhang, C. Pd-Catalyzed Stereoselective 1, 2-Arylboration of Alkenylarenes. *Org. Lett.* **2019**, *21*, 8106–8109.
- (54) Nelson, H. M.; Williams, B. D.; Miró, J.; Toste, F. D. Enantioselective 1, 1-arylborylation of alkenes: merging chiral anion phase transfer with Pd catalysis. *J. Am. Chem. Soc.* **2015**, *137*, 3213–3216.
- (55) Shen, H. C.; Wang, P. S.; Tao, Z. L.; Han, Z. Y.; Gong, L. Z. An enantioselective multicomponent carbonyl allylation of aldehydes with dienes and alkynyl bromides enabled by chiral palladium phosphate. *Adv. Synth. Catal.* **2017**, *359*, 2383–2389.
- (56) Nimmagadda, S. K.; Liu, M.; Karunananda, M. K.; Gao, D. W.; Apolinar, O.; Chen, J. S.; Liu, P.; Engle, K. M. Catalytic, Enantioselective  $\alpha$ -Alkylation of Azlactones with Nonconjugated Alkenes by Directed Nucleopalladation. *Angew. Chem., Int. Ed.* **2019**, *58*, 3923–3927.
- (57) Lim, C. S.; Quach, T. T.; Zhao, Y. Enantioselective Synthesis of Tetrahydroquinolines by Borrowing Hydrogen Methodology: Cooperative Catalysis by an Achiral Iridacycle and a Chiral Phosphoric Acid. *Angew. Chem., Int. Ed.* **2017**, *56*, 7176–7180.
- (58) Rajkumar, S.; He, S.; Yang, X. Kinetic Resolution of Tertiary 2-Alkoxy-carboxamido-Substituted Allylic Alcohols by Chiral Phosphoric Acid Catalyzed Intramolecular Transesterification. *Angew. Chem., Int. Ed.* **2019**, *58*, 10315–10319.
- (59) Huang, B.; He, Y.; Levin, M. D.; Coelho, J. A.; Bergman, R. G.; Toste, F. D. Enantioselective Kinetic Resolution/Desymmetrization of Para-Quinolins: A Case Study in Boronic-Acid-Directed Phosphoric Acid Catalysis. *Adv. Synth. Catal.* **2020**, *362*, 295–301.
- (60) Mao, Y.; Wang, Z.; Wang, G.; Zhao, R.; Kan, L.; Pan, X.; Liu, L. Redox deracemization of tertiary stereocenters adjacent to an electron-withdrawing group. *ACS Catal.* **2020**, *10*, 7785–7791.
- (61) McLean, L. A.; Ashford, M. W.; Fyfe, J. W.; Slawin, A. M.; Leach, A. G.; Watson, A. J. Asymmetric synthesis of heterocyclic chloroamines and aziridines by enantioselective protonation of catalytically generated enamines. *Chem. -Eur. J.* **2022**, *28*, e202200060.
- (62) Wang, S.; Arguelles, A. J.; Tay, J. H.; Hotta, M.; Zimmerman, P. M.; Nagorny, P. Experimental and computational studies on regio-divergent chiral phosphoric acid catalyzed cycloisomerization of mupirocin methyl ester. *Chem. -Eur. J.* **2020**, *26*, 4583–4591.
- (63) Featherston, A. L.; Kwon, Y.; Pompeo, M. M.; Engl, O. D.; Leahy, D. K.; Miller, S. J. Catalytic asymmetric and stereodivergent oligonucleotide synthesis. *Science* **2021**, *371*, 702–707.
- (64) Han, Z.; Zang, Y.; Liu, C.; Guo, W.; Huang, H.; Sun, J. Enantioselective synthesis of triarylmethanes via organocatalytic transfer hydrogenation of para-quinone methides. *Chem. Commun.* **2022**, *58*, 7128–7131.
- (65) Li, X.; Duan, M.; Deng, Z.; Shao, Q.; Chen, M.; Zhu, G.; Houk, K. N.; Sun, J. Catalytic enantioselective synthesis of chiral tetraaryl-methanes. *Nature Catalysis* **2020**, *3*, 1010–1019.
- (66) Sun, G.; Deng, Z.; Luo, Z.; Wang, Z.; Zhang, J. Organocatalytic Asymmetric Arylation of p-Quinone Phosphonates: A Green Access to Biaryl Monophosphorus Ligands. *Org. Lett.* **2021**, *23*, 7630–7634.
- (67) Lv, C.; Xu, G.; Yang, R.; Zhou, L.; Wang, Q. Stereodivergent polycaprolactones formed by asymmetric kinetic resolution polymerization of 6-methyl- $\epsilon$ -caprolactone. *Polym. Chem.* **2021**, *12*, 4856–4863.
- (68) Ye, X.; Pan, Y.; Chen, Y.; Yang, X. Enantioselective Construction of Sulfur-Containing Tetrasubstituted Stereocenters via Asymmetric Functionalizations of  $\alpha$ -Sulfanyl Cyclic Ketones. *Adv. Synth. Catal.* **2020**, *362*, 3374–3379.
- (69) Li, F.; Liang, S.; Luan, Y.; Chen, X.; Zhao, H.; Huang, A.; Li, P.; Li, W. Organocatalytic regio-, diastereo- and enantioselective  $\gamma$ -additions of isoxazol-5 (4 H)-ones to  $\beta$ ,  $\gamma$ -alkynyl- $\alpha$ -imino esters for the synthesis of axially chiral tetrasubstituted  $\alpha$ -amino allenolates. *Org. Chem. Front.* **2021**, *8*, 1243–1248.
- (70) Romanov-Michailidis, F.; Romanova-Michaelides, M.; Pupier, M.; Alexakis, A. Enantioselective Halogenative Semi-Pinacol Rearrangement: Extension of Substrate Scope and Mechanistic Investigations. *Chem. -Eur. J.* **2015**, *21*, 5561–5583.
- (71) Romanov-Michailidis, F.; Guénee, L. and Alexakis, A. Enantioselective Organocatalytic Fluorination-Induced Wagner–Meerwein Rearrangement. *Angew. Chem., Int. Ed.* **2013**, *52*, 9266–9270.
- (72) Avila, C. M.; Patel, J. S.; Reddi, Y.; Saito, M.; Nelson, H. M.; Shunatona, H. P.; Sigman, M. S.; Sunoj, R. B.; Toste, F. D. Enantioselective Heck–Matsuda arylations through chiral anion phase-transfer of aryl diazonium salts. *Angew. Chem., Int. Ed.* **2017**, *56*, 5806–5811.
- (73) Meng, J.; Li, X. H.; Han, Z. Y. Enantioselective hydroaminomethylation of olefins enabled by Rh/Bronsted acid relay catalysis. *Org. Lett.* **2017**, *19*, 1076–1079.
- (74) Wang, D.; Liu, W.; Tang, M.; Yu, N.; Yang, X. Atroposelective synthesis of biaryl diamines and amino alcohols via chiral phosphoric acid catalyzed para-aminations of anilines and phenols. *iScience* **2019**, *22*, 195–205.
- (75) Rauniyar, V.; Wang, Z. J.; Burks, H. E.; Toste, F. D. Enantioselective synthesis of highly substituted furans by a copper (II)-catalyzed cycloisomerization–indole addition reaction. *J. Am. Chem. Soc.* **2011**, *133*, 8486–8489.
- (76) Pedrazzani, R.; An, J.; Monari, M.; Bandini, M. New Chiral BINOL-Based Phosphates for Enantioselective [Au(I)]-Catalyzed Dearomatization of  $\beta$ -Naphthols with Allenamides. *Eur. J. Org. Chem.* **2021**, *11*, 1732–1736.
- (77) Romano, C.; Jia, M.; Monari, M.; Manoni, E.; Bandini, M. Metal-Free Enantioselective Electrophilic Activation of Allenamides: Stereoselective Dearomatization of Indoles. *Angew. Chem., Int. Ed.* **2014**, *53*, 13854–13857.



- (78) Cui, L.; You, Y.; Mi, X.; Luo, S. Asymmetric Fluorination of  $\alpha$ -Branched Aldehydes by Chiral Primary Amine Catalysis: Reagent-Controlled Enantioselectivity Switch. *J. Org. Chem.* **2018**, *83*, 4250–4256.
- (79) Shibatomi, K.; Okimi, T.; Abe, Y.; Narayama, A.; Nakamura, N.; Iwasa, S. Organocatalytic asymmetric fluorination of  $\alpha$ -chloroaldehydes involving kinetic resolution. *Beilstein J. Org. Chem.* **2014**, *10*, 323–331.
- (80) Shibatomi, K.; Yamamoto, H. Stereoselective Synthesis of  $\alpha,\alpha$ -Chlorofluoro Carbonyl Compounds Leading to the Construction of Fluorinated Chiral Quaternary Carbon Centers. *Angew. Chem., Int. Ed.* **2008**, *47*, 5796–5798.
- (81) Witten, M. R.; Jacobsen, E. N. A Simple Primary Amine Catalyst for Enantioselective  $\alpha$ -Hydroxylations and  $\alpha$ -Fluorinations of Branched Aldehydes. *Org. Lett.* **2015**, *17*, 2772–2775.
- (82) Gallegos, L. C.; Luchini, G.; St John, P. C.; Kim, S.; Paton, R. S. Importance of Engineered and Learned Molecular Representations in Predicting Organic Reactivity, Selectivity, and Chemical Properties. *Acc. Chem. Res.* **2021**, *54*, 827–836.
- (83) Shibatomi, K.; Kitahara, K.; Okimi, T.; Abe, Y.; Iwasa, S. Enantioselective fluorination of  $\alpha$ -branched aldehydes and subsequent conversion to  $\alpha$ -hydroxyacetals via stereospecific C–F bond cleavage. *Chem. Sci.* **2016**, *7*, 1388–1392.

#### TOC Graphic

